Naval Surface Warfare Center
Carderock Division
West Bethesda, MD 20817-5700

NSWCCD-61-TR–2011/04 February 2011

Survivability, Structures, and Materials Department

Technical Report

Nondestructive Examination of Aluminum Friction Stir Welds: A Literature Search

by

Nathan Trepal and Maria Posada

Naval Surface Warfare Center
Carderock Division
West Bethesda, MD 20817-5700

NSWCCD-61-TR–2011/04 February 2011

Survivability, Structures, and Materials Department

Technical Report

Nondestructive Examination of Aluminum Friction Stir Welds: A Literature Search

by

Nathan Trepal and Maria Posada

REPORT DOCUMENTATION PAGE

Form Approved
OMB No. 0704-0188

1. REPORT DATE *(DD-MM-YYYY)*	2. REPORT TYPE	3. DATES COVERED *(From - To)*
3-Feb-2011	Final	-

4. TITLE AND SUBTITLE
Nondestructive Examination of Aluminum Friction Stir Welds: A Literature Search

5a. CONTRACT NUMBER

5b. GRANT NUMBER

5c. PROGRAM ELEMENT NUMBER

6. AUTHOR(S)
Nathan Trepal and Maria Posada

5d. PROJECT NUMBER

5e. TASK NUMBER

5f. WORK UNIT NUMBER

7. PERFORMING ORGANIZATION NAME(S) AND ADDRESS(ES) AND ADDRESS(ES)

Naval Surface Warfare Center
Carderock Division
9500 Macarthur Boulevard
West Bethesda, MD 20817-5700

8. PERFORMING ORGANIZATION REPORT NUMBER

NSWCCD-61-TR-2011/04

9. SPONSORING / MONITORING AGENCY NAME(S) AND ADDRESS(ES)

10. SPONSOR/MONITOR'S ACRONYM(S)

11. SPONSOR/MONITOR'S REPORT NUMBER(S)

12. DISTRIBUTION / AVAILABILITY STATEMENT
Approved for public release; distribution is unlimited.

13. SUPPLEMENTARY NOTES

14. ABSTRACT
The purpose of this report is to provide a review of available information on friction stir welding (FSW) defects and the nondestructive examination (NDE) methods currently used to detect these defects. The report is divided into three sections in order to best present its findings. The first section, "Friction Stir Welding (FSW) Defects and Characteristics," identifies the defects and discusses detection methods used in detecting each defect. The second section, "Quality Assurance Evaluation Techniques," discusses the various detection methods available for detecting FSW defects. It analyzes the conventional NDE methods, newer NDE methods, and other methods, including destructive testing and in-process monitoring, used in assuring the quality of friction stir welds. The final section is "Industry Documents." This last section describes documents and associated requirements invoked by industry to evaluate friction stir welds.

15. SUBJECT TERMS
Friction Stir Welding Nondestructive Examination Nondestructive Evaluation
Nondestructive Inspection Nondestructive Testing Aluminum Alloys

16. SECURITY CLASSIFICATION OF:			17. LIMITATION OF ABSTRACT	18. NUMBER OF PAGES	19a. RESPONSIBLE PERSON
a. REPORT	b. ABSTRACT	c. THIS PAGE			Nathan Trepal
UNCLASSIFIED	UNCLASSIFIED	UNCLASSIFIED	SAR	46	19b. TELEPHONE NUMBER *(include area code)* 301.227.5144

Contents

Page
Contents iii
Figures v
Tables vii
Administrative Information viii
Abstract ix
1 Background 1
1.1 Friction Stir Welding 1
1.2 FSW of 5xxx Series Aluminum Alloys 2
2 Friction Stir Welding Defects and Characteristics 4
2.1 Dimensional Variation 4
2.2 Excessive Flash 4
2.3 Chevron Markings 4
2.4 Faying Surface Indications 5
2.5 Porosity 5
2.6 Wormholes 5
2.7 Root Flaws 5
2.8 Kissing Bonds 6
2.9 Pin Tool Loss 7
2.10 Residual Stresses 7
3 Quality Assurance Evaluation Techniques 9
3.1 Nondestructive Examination 9
3.1.1 Conventional Methods 9
3.1.1.1 Visual Testing 9
3.1.1.2 Dye Penetrant Testing 9
3.1.1.3 Eddy Current Testing 9
3.1.1.4 Radiographic Testing 10
3.1.1.5 Ultrasonic Testing 10
3.1.2 Advanced NDE Methods 11
3.1.2.1 Phased-Array Ultrasonic Testing 11
3.1.2.2 Acoustic Emission 12

3.1.2.3 Multi-Element Eddy-Current 12
3.1.2.4 Transient Eddy Current Inspection 13
3.1.2.5 Holography & Shearography 13
3.1.3 Calibration Standards 14
3.2 Destructive Testing 14
3.3 In-Process Monitoring 14
4 Industry Documents 15
4.1 Lloyd's Register of Shipping 15
4.2 NASA Process Specification for Friction Stir Welding 16
4.3 Other Industry Guidelines 17
5 Summary 18
References 19
Distribution 35

Figures

Page

Figure 1. Schematic of FSW process sequence. (a) Rotating tool above joint; (b) Rotating tool lowered onto joint line; (c) Z-axis load drives rotating pin into the joint creating frictional heat; (d) X-axis load is applied causing the rotating tool to traverse along the joint line. 22
Figure 2. Some FSW terminology [10]..... 22
Figure 3. A 6mm thick AA 2014A FS weld cross-section. The increments at the bottom of the image are each 1mm [10]. 23
Figure 4. Some possible FSW hardness profiles along a given plane lying parallel to the crown and root of the weld. (b) schematically represents an FS welded AA 5083-H131 hardness profile and (d) schematically represents an FS welded AA 5083-O hardness profile [5]. 23
Figure 5. Grain size distribution at various locations within an AA 7050 weld nugget [2]. 24
Figure 6. An FS welded aluminum alloy with excessive flash. 24
Figure 7. Chevron markings found on the root side of an AA 5083 FS weld. 1mm increments run along the bottom of the image [10]. 25
Figure 8. Chevron markings found on the root side of an AA 5251 FS weld. 1mm increments run along the bottom of the image [10]. 25
Figure 9. Macroscopic etch showing a faying surface defect, void, and LOP defect [28]. 26
Figure 10. An FS welded aluminum alloy containing a surface-breaking wormhole defect. 26
Figure 11. Optical micrograph of a root flaw in an AA 2024-T3 FS weld, after etching [34]. 27
Figure 12. (a) Cross-section perpendicular to the welding direction of an etched AA 5083 FS weld and (b) an optical micrograph of the black-square region in (a). Notations “R.S.” and “A.S.” in (a) stand for “retreating side” and “advancing side” of the welding tool, respectively [18]. 27
Figure 13. Fatigue data and corresponding S–N curves of AA 5083 kissing bonded and sound welds [18]. 28
Figure 14. Effect of welding parameters on the formation of a visible zigzag line (upon etching) and kissing bond in an FSW AA 1050 weld [17]. 28
Figure 15. (A) Schematic showing test specimens created with known size and location for boreholes (top) and EDM notches representing elliptical cracks (bottom) within an aluminum alloy, (B) schematic showing 0º and 20º inspection angles (in

water) evaluated for inspection of lack of penetration and volumetric defects, such as voids, and (C) showing (top scan) ultrasonic C-scan results for borehole echoes and (bottom scan) showing a B-scan (side view of the boreholes) [26]. 29
Figure 16. UT inspection results using 25 MHz transducer at 0º incidence of defects in 4-mm thick FS welded aluminum alloy - top: shows a C-scan of the defect echo, center: shows a C-scan of the backwall echo, and the bottom: shows a D-scan (time of flight) echo. From the signal amplitude in the D-scan above and information regarding sound velocity of longitudinal waves in this aluminum alloy (6100 m/s), the author was able to roughly position the volumetric defect within the upper half of the 4-mm thick plate [26]. 30
Figure 17. (A) Schematic showing two transducer configuration (transmitter/receiver and receiver) and a single transducer that transmits and receives; both using diagonal incidence (B) C-scan showing echo of elliptical crack in 6 mm thick aluminum plate using a *focused* 25 MHz transducer and a 20º angle of incidence in water (C) C-scan of same 6-mm thick aluminum plate but this time using an *unfocused* 10 MHz transducer at a 20º angle of incidence in water [26]. 31
Figure 18. D-Scan (time-of-flight) showing a root gap detected by ultrasonic inspection in 6-mm thick aluminum alloy that was not detected by visual inspection. This scan was produced using a single focused 25 MHz transducer at an angle of 20º in water [26]. 31
Figure 19. Locations of test coupons for qualification of welding procedures for LR's Guidelines for Approval of FS welds [11]. 32

Tables

Page

Table 1. Key Benefits of FSW [2] 33

Table 2. A summary of A.J. Leonard's x-ray and ultrasonic inspection results for each of the alloy 2014A FS welds. As can be seen when analyzing the columns, for many of the weld samples, RT and UT were unable to detect defects found through destructive analysis [10]..... 33

Table 3. A qualitative summary of detectability of various defects at various angles using phased-array UT. As can be seen in this matrix, a combination of the 35° and 65° refracted angles would have been able to detect all the defects [7]..... 34

Administrative Information

This report was prepared by the Welding, Processing, and NDE Branch (Code 611) of the Naval Surface Warfare Center, Carderock Division (NSWCCD). The work was funded by the Office of Naval Research, Manufacturing Technology Program. This report also represents the deliverable for Task 2a of the LHA 6 Friction Stir Welding Process and Application Program (TI 3331-0013). The authors would also like to acknowledge the help and contributions from the many individuals listed in the references section, many of whom were contacted personally, as well as the help and contribution of Kirsten Green, NAVSEA 05P2.

Abstract

The purpose of this report is to provide a review of available information on friction stir welding (FSW) defects and the nondestructive examination (NDE) methods currently used to detect these defects. The report is divided into three sections in order to best present its findings. The first section, "Friction Stir Welding (FSW) Defects and Characteristics," identifies the defects and discusses inspection methods used in detecting each defect. The second section, "Quality Assurance Evaluation Techniques," discusses the various detection methods available for detecting FSW defects. It analyzes the conventional NDE methods, newer NDE methods, and other methods, including destructive testing and in-process monitoring, used in assuring the quality of friction stir welds. The final section is "Industry Documents." This last section describes documents and associated requirements invoked by industry to evaluate friction stir welds.

1 Background

The U.S. Navy is using friction stir welding (FSW) to fabricate 5xxx series, and possibly 6xxx series, aluminum structures for both LCS and LHA-6. In both applications, FSW is being evaluated as a replacement for conventional gas metal arc welding (GMAW). While there has been considerable advancement in FSW of aluminum structures and successful implementation within the aerospace community, little work has been performed to establish its adequacy for naval ship applications. Among the most critical needs in this regard are: (1) determining if the mechanical, material, and corrosion properties of FS welded aluminum are adequate for service; (2) establishing weld procedure and performance qualification requirements; and (3) developing fabrication and inspection requirements.

This document addresses inspection of FS welds. It provides results of literature and industry surveys conducted to determine the types of discontinuities and inspection methods typically associated with aluminum FS welds.

1.1 Friction Stir Welding

Friction stir welding is a solid-state welding process invented by TWI in 1991. As shown in Figure 1, the process begins when a rotating welding tool, consisting of a cylindrical shoulder with a profiled pin, is lowered and brought into contact with the base material to be joined. The base material is typically clamped onto a backing bar in a manner that prevents the abutting joint faces from being forced apart. As the welding tool is rotating, a force (z-axis load) is applied perpendicular to the joint line that drives the pin into the workpiece and creates frictional heating. After sufficient dwell time, another force (x-axis load) is applied in the direction of travel. Both z- and x-axis loads act on the tool as the rotating welding tool traverses along the joint line. The action of the tool shoulder in contact with the surface and the pin within the base material creates frictional heat, which softens, but does not melt, the material. The softened material moves around the periphery of the pin and is deposited behind the pin. The “stirring” action and pressure applied by both the tool and fixturing create a highly-deformed, plasticized material that is consolidated upon cooling to create a bond. As the rotating material stirs the metal, material on one side of the tool is pushed forward in the direction of tool travel. Material on the other side is pushed backward, in the opposite direction of tool travel. The side in which material is pushed forward is known as the “advancing side.” The side in which material is pushed backward is known as the “retreating side.” The difference in material movement results in an asymmetrical microstructure. Figure 2 is a schematic defining some of the FSW terminology used for a welded component. Figure 3 shows a cross-sectional view of an AA 2014A FS welded microstructure.

Friction stir welding is now beginning to be accepted for many industrial applications. The aerospace industry has been one of the primary implementers of the technology, including use by Boeing, Lockheed Martin, NASA, and Eclipse Aviation to bring the technology into commercial applications. Friction stir welding is also being utilized for high-speed trains and in the automotive industry for engine and chassis

cradles, truck bodies, tail lifts for lorries, mobile cranes, armor plate vehicles, and fuel tankers [1].

Numerous aluminum alloys, the metal initially tested and developed for the FSW process, have been successfully FS welded. Wrought aluminum alloys have been tested in thicknesses from less than 1 mm up to 75 mm, typically using tool steel for the pin tool material [1]. Aluminum alloys of 1xxx, 2xxx, 5xxx, 6xxx, 7xxx series have seen extensive testing with FSW.

Friction stir welding consumes less energy than conventional welding methods and no gas or flux is used, making the process more environmentally friendly. Also, the joining does not require any filler metal, alleviating many compatibility issues with composition, which can be an issue in traditional welding [2].

Table 1 shows some of the key benefits of FSW. Because FSW is a solid-state process, it does not create weld defects found in fusion welds, such as liquation cracking, solidification cracking, and oxide formation. It also has been shown to have a lower propensity for thermal distortion and high residual stresses [3], and has produced structural joints with higher strength, increased fatigue life, and less sensitivity to corrosion compared to conventional arc welds for particular aluminum alloys [4].

1.2 FSW of 5xxx Series Aluminum Alloys

The influence of welding on aluminum alloys depends a great deal on whether the alloy is a heat-treatable grade or a non-heat treatable grade. Heat treatable grades, such as the 6xxx series alloys, suffer large degradation in properties because the heat of welding essentially destroys the heat treated structure. The consequence is that the heat-affected-zone (HAZ) of a 6xxx series weldment can be significantly softer than the parent metal. Due to the differences in thermal cycles, this effect, though present, typically is much less pronounced in FS welds than in arc welds.

Non-heat treatable grades, such as 5xxx alloys, do not rely on heat treatment as the primary strengthening tool and thus the strength loss in the weld and HAZ regions is much less pronounced. In fact, for 5xxx series aluminum alloys, which rely on cold work for strengthening, it can either generate a softer weld nugget and HAZ than the parent material (such as FS welded AA 5083-H131) or a harder, cold-worked weld nugget than the parent material (such as FS welded AA 5083-O). Figure 4 schematically represents these possible variations. Figure 5 shows the grain size distribution at various locations within an AA 7050 weld nugget. Because of the asymmetry of the weld zones with respect to the weld centerline and mid-thickness plane, the hardness distribution will vary with depth. That is, the hardness of FS welds varies from near the face, through the mid-thickness, to the root of the weld. An asymmetrical hardness variation also exists across the cross-sectional joint profile, from advancing side to retreating side [5].

The microstructural variation and asymmetry of FS welds are due to the rotational nature of FSW and the tool geometry. Measurements taken during actual FSW reveal that the temperatures of the advancing and retreating sides are not the same [5]. In another example, relating specifically to the effect of tool geometry in creating welding

defects, Colligan and Creeden determined that excess shoulder diameter to pin diameter ratios induced welding defects [6]. This suggests that any changes in tool design will require a thorough requalification of all the FSW parameters for a process.

Friction stir welding is highly automated, with several process variables, some of which are different from those encountered in conventional welding. These variables include, but are not limited to, tool rotational speed, tool rotational direction, tool design and material, tool tilt angle, welding force, materials, plunge depth, travel speed, and penetration depth. It should be noted that even with strict control on all of the process variables, joint properties would vary as a function of the composition and grain structure at the location of the weld. This means that, like conventional arc welding, microstructure and joint properties can vary from plate to plate. This also means that, due to differences in composition and processing, a given 5xxx series alloy from different producers can result in different joint properties [5].

2 Friction Stir Welding Defects and Characteristics

Friction stir welding produces defects of different orientations and skews [7]. Although FSW defects may be in potentially any orientation, most lie along the axial and transverse axes [8]. Thus, while there are some defects that are difficult to detect through conventional nondestructive examination (NDE) methods, most are in an adequate orientation, making sensitivity the only issue in detecting the majority of the FSW defects. For defects that are difficult to detect by conventional means, industry has relied on in-process monitoring, destructive testing, novel NDE methods, or some combination of these to mitigate the risk associated with those defects.

A list and description of various characteristics of FS welds are listed below. Within this list are defects typically encountered and inspected for that result from non-optimized process controls during FSW. These defects include volumetric defects, lack of penetration (LOP) defects, and kissing bonds. Volumetric defects are detectable by conventional NDE techniques. Lack of penetration defects are detectable by conventional NDE techniques, with some additional surface preparation prior to inspection. The kissing bond, is much more difficult to detect by conventional ultrasonic inspection and radiographic inspection due to the nature of this type of defect.

2.1 Dimensional Variation

Residual stresses have been found to be lower than those created during conventional welding, resulting in less dimensional variation after welding has finished. However, Dickerson and Przydatek found that the thickness of the parent plate is a key parameter in both the flaw size and degradation of weld performance. The pair note that a tolerance of +0.2 mm over the nominal thickness is the general rule given by The Welding Institute and suggested by Lloyd's Register of Shipping [9] to ensure adequate joint quality. Any postweld dimensional changes can be measured through visual inspection and other methods used for conventional welds.

2.2 Excessive Flash

Flash is produced by displacement of material from the mating components caused by the pin tool being plunged into the materials. If the insertion depth is too deep, the tool plunges into the weld joint creating excessive flash. This may result in a significantly concave weld, causing local thinning of the welded plates [2]. Figure 6 shows an example of an FS welded aluminum alloy with excessive flash. This condition can be detected visually and through in-process monitoring. The flash can then be machined off to meet surface finish requirements for the part.

2.3 Chevron Markings

Leonard [10] found chevron markings on the root side of FS welded AA 5083-O and FS welded AA 5251-H22 (1/4 hard), but the properties of the welds appeared unaffected (see Figure 7 and Figure 8). Lloyd's Register of Shipping *Guidelines for Approval of Friction Stir Welding* includes concern that the presence of chevron markings may reduce corrosion resistance [11], but no data were found to confirm this. Chevron

markings, sometimes called a herring bone pattern, can be detected visually, but can interfere with dye penetrant analysis (in which case grinding, machining, or etching the surface to facilitate analysis may be acceptable).

2.4 Faying Surface Indications

Surface galling, or faying surface indications occur on the top surface of a weld and are caused by the rubbing of abutting faces of the parent material which generally appears as a small lap. Figure 9 shows a macroscopic etch with a faying surface defect. This type of indication is near the top surface and can be removed with minimal machining or perhaps etching. The criticality of this flaw is unknown since little is written about this type of indication. The literature does not indicate whether conventional NDE methods can reliably detect this type of indication. The Lloyd's Register of Shipping *Guidelines for Approval of Friction Stir Welding*, which calls the defect a cold lap, states that it can interfere with dye penetrant testing [11]. NASA and Lockheed Martin have mentioned success in identifying faying surface indications with phased-array ultrasonic testing (UT) [12]. It is believed that these indications may also be detectable through destructive testing and in-process monitoring.

2.5 Porosity

Chen's group, in studying the joining of AA 6061 to AISI 1018 steel by FSW, found numerous pores were exposed at the top of the weld along the centerline at and near the start of the welding pass. The group also found porosity increased near the root of the weld as tool wear increased [13]. Insufficient forging pressure, excessive travel speed, and/or too large a root gap may cause the formation of voids [10].

Conventional radiographic testing (RT) and ultrasonic testing (UT) can detect voids of a detectable size. Phased-array UT also has proven capable of detecting voids [12]. Destructive testing and in-process monitoring should also prove capable in void detection.

2.6 Wormholes

Wormholes are single voids extending longitudinally along the weld. Wormholes may be surface breaking or contained entirely within the volume of the weld. Lack of forging defect is a term that is sometimes used to describe an FSW defect, but it is believed to be equivalent to a wormhole defect [14]. Figure 10 shows a wormhole which has opened to the surface.

Wormholes are readily detected by conventional NDE [7]. NASA and Lockheed Martin have found conventional UT can detect the start of a wormhole better than radiographic testing (RT), but both are successful in detecting this anomaly [12]. Destructive testing and phased-array UT will also uncover this defect. In-process monitoring may possibly be used in the prevention or detection of this defect, as well.

2.7 Root Flaws

Full closure of the root necessitates the pin to pass very close to the backing plate, since only a limited amount of deformation and material flow occurs below the pin tip.

Plus, the deformation at the pin tip only occurs close to the pin tip surface [5]. Root flaws, such as LOP flaws, result when the pin does not pass close enough to the backing plate to allow a complete bond to be formed along the entire plane of the abutting surfaces. Figure 11 shows an etched example of a root flaw.

Dickerson and Przydatek found that visual testing (VT), dye penetrant (PT), and RT are not reliable in finding root flaws, despite having root bend tests confirm the presence of the flaws [9]. NASA found that VT and PT can find such flaws if the root area is etched prior to inspection [15].

Aside from post-etched VT and PT, phased-array UT, multi-element eddy current testing, and transient eddy current testing are also capable NDE methods in detecting root flaw defects. In-process monitoring may also be capable in detecting this flaw. Destructive bend testing can confirm the presence of this flaw. Machining the root is also effective in removing some root flaws [10].

2.8 Kissing Bonds

Khaled uses Oosterkamp's definition of kissing bonds as "two surfaces lying extremely close together, but not close enough for the majority of the original surface asperities to have deformed sufficiently to affect the formation of atomic bonds" [5]. The use of this definition, allows a kissing bond to be defined as a tight LOP, or root flaw. This is what Stepinski does within his report [16].

Sato calls a kissing bond a defect associated with remnants of the initial oxide layer on the abutting surfaces of an FS weld, remaining as a faint zigzag-line pattern on the cross section, which adversely affects the mechanical properties of the weld [17]. This definition is more in-line with many of the definitions describing joint line remnants (JLR), entrapped oxides, residual oxides, and lazy-S curves.

This report uses Sato's definition for kissing bonds. Any references to Stepinski's kissing bond are described as an LOP or root flaw.

Figure 12 shows an etched cross-section of a kissing bond located within an AA 5083 FS weld. Depending on location and extent, kissing bonds can have a deleterious effect on fatigue life, impact strength, and through-thickness load-bearing capacity [5].

Zhou et al. reported that kissing bonds reduce the fatigue life of FS welds in both low-cycle and high-cycle fatigue, but especially in the former [18]. Figure 13 shows fatigue data obtained for AA 5083. The group found the fatigue life of AA 5083 FS welds with kissing bonds, in the form of oxide arrays, to be 20 – 40 times less than the fatigue lives of sound welds, under the stress ratio R = 0.1. For example, compared to sound FS welds, the fatigue properties of the AA 5083 FS welds with kissing bonds were reduced by 35% at 2 x 10^6 cycles [18].

Sato et al. studied the kissing bond in AA 1050 [17]. The study found no defects by either PT or VT in the as-polished cross-section. However, etching in an NaOH aqueous solution, preferentially etched the zigzag oxide-line in the stir zone of all the welds

except those produced at the higher heat-input parameters (a combination of higher rotational speed and lower traverse speed) [17]. Figure 14 shows the results of the study for each of the welds analyzed.

One proposed cause of this type of discontinuity is that inadequate pre-weld cleaning may result in insufficient dispersion of oxides built up along the joint line [10]. NASA and Lockheed Martin have found that, with 2xxx series aluminum alloys, allowing the plates to wait 14 – 21 days between cleaning and welding allows enough oxide to build up on the abutting surfaces to develop a residual oxide layer/interface within the workpiece after FSW. NASA has only found kissing bonds within components FS welded with a self-reacting pin tool and not with a fixed pin tool [12]. NASA also found that phased-array UT is capable of detecting the flaw, if it is of a detectable size. Poor tool-to-joint alignment, insufficient pin depth, or tool plunge depth may also cause kissing bonds due to inadequate disruption of oxides present along the abutting parent materials. Cleaning or machining the abutting faces just prior to welding should avoid this problem [10].

Kissing bonds are difficult to detect by conventional NDE methods due to the defect's tight nature [7] and because these flaws are formed from oxides on abutting surfaces prior to welding, in-process monitoring is of little aid. Destructive testing and phased-array UT have proven capable of detecting this type of flaw.

2.9 Pin Tool Loss

In FSW, tool geometry greatly impacts joint profiles and the features within the weld zone [5]. The tool's primary functions are to induce localized heating and material flow [2]. Thus, the loss of pin tool material during FSW can have a large impact on weld quality if pin loss is not identified during welding or if the pin tool remains embedded within the weld nugget.

For all common aluminum alloys of thicknesses less than 12 mm, AISI-H13 and AISI-M42 tools steels are typical materials used as pin tools in commercial FSW production. Creep and creep fatigue are potential concerns for tool life in aluminum FSW for weld lengths of over 1 km [19]. NASA and Lockheed Martin have been able to detect broken tool chips by RT [14].

The criticality of pin tool life with respect to wear has also been noted by the Air Force. They have observed substantial tool wear when FS welding 5xxx series aluminum alloys that can contribute to stress corrosion cracking (SCC) concerns. A tool maintenance program with tight tolerances is required to maintain consistent weld quality [20]. Depending on the size of the remnant pin tool pieces, RT, UT, and phased-array UT are capable of detecting these defects. In-process monitoring may also be able to identify when pin tool loss occurs during welding [21] and may be identifiable by destructive testing.

2.10 Residual Stresses

Residual stresses are believed to be lower in FS welds than in conventional arc welds because the FSW process is solid-state; however, the rigid clamping used in FSW

exerts a much higher restraint on the welded plates than the compliant clamps used for fixing parts during conventional welding. Mishra and Ma noted that "these restraints impede the contraction of the weld nugget and heat-affected zone during cooling in both longitudinal and transverse directions," generating residual stresses. These stresses could significantly affect post weld mechanical properties; particularly fatigue strength [2].

The experimental work of Fratini and Zuccarello [22] found residual stresses to be different from those found in conventional arc welded joints, where the maximum residual stress values occur close to the surface (this would be near the tool shoulder border of the advancing side for an FSW joint). In FS welded joints created with a tool tilt of 2°, residual stresses take a general negative value at the surface and become positive within the joint. Fratini and Zuccarello found the maximum residual stresses to be less than those found in conventionally arc-welded joints [22].

Work by James and Mahoney on measuring residual stresses in FS welded AA 7050-T7451, C458 Al-Li alloy, and AA 2219 by x-ray diffraction $\sin^2 \psi$ method found that longitudinal (parallel to the welding direction) residual stresses were generally tensile and transverse (normal to the welding direction) residual stresses were generally compressive [2].

Friction stir welded AA 2024-T3 and AA 6013-T6 longitudinal residual stresses were always found to be higher than the transverse residual stresses – independent of pin diameter, tool rotation rate, and traverse speed – when analyzed by cut compliance technique, x-ray diffraction, neutron diffraction, and high-energy synchrotron radiation by Donne et al. Both Donne et al. and Peel et al. found the maximum tensile stresses to be located approximately 10 mm away from the weld centerline, in the heat affected zone (HAZ). This distance corresponded with the edge of the tool shoulder. Peel et al. found that longitudinal residual stresses increased with an increasing pin tool traverse speed, but that transverse residual stresses were independent of the pin tool traverse speed [2].

Maximum residual stresses from various FS welds of aluminum alloys were below 100 MPa, significantly lower than fusion welds and respective yield stresses of these alloys, resulting in a significant reduction of distortion in the parent plates [2]. Also, experimental work has been performed in attempting to reduce tensile residual stresses in FS welds through the application of mechanical tensioning during the FSW process. While the work has shown an ability to induce large compressive stresses, much work is still needed before it can be applied to an industrial process [23].

There are nondestructive methods available in identifying residual stresses, some of which are briefly discussed in the "Advanced NDE Methods" section.

3 Quality Assurance Evaluation Techniques

3.1 Nondestructive Examination

3.1.1 Conventional Methods

Industrial practice has shown that the following NDE methods are reliable in finding defects of approximately 0.25 in or greater within FS welds [12], [20]. While these methods may be called conventional within this report, their ability to detect FSW discontinuities may be greatly affected by implementing non-standard practices in their usage. For instance, visual testing (VT) and dye penetrant testing (PT) typically require some surface removal prior to inspecting the root of the weld and the references to conventional ultrasonic testing (UT) are all for immersion UT only.

3.1.1.1 Visual Testing

Industry has used VT to identify an adequate "as-machined" appearance of the weld, dimensional checks, excessive flash, and in the identification of chevron-markings. Used in combination with etching, visual inspection has also been successfully used to identify root flaws [15].

3.1.1.2 Dye Penetrant Testing

Dye penetrant testing (PT) can be used for the detection of surface-breaking defects with some volume associated with the defect. Examples of surface-breaking volumetric defects include oblong voids and LOP. At NASA, PT has only been found to be reliable for detecting root flaws when the root has been etched prior to inspection [12].

Stepinski [16] reports that penetrant root-side inspections of as-welded material proved unsuccessful due to interference of existing surface features on the root side that rendered poor detectability. Similar to NASA, the author reports that penetrant inspection carried out for surface breaking flaws on the root-side of FS welds is improved when an etchant was used to remove a minimum amount of material (approximately 0.004 in). The etchant allowed discrimination of these root side flaws by observing microstructural differences. In addition, the author comments that double etching using a caustic etchant solution further improved the detection of LOP flaws. Note that differences exist in penetrant solutions that result in differing sensitivities to surface flaw detection.

3.1.1.3 Eddy Current Testing

Depth of penetration is limited in eddy current testing (ET) since sensitivity decreases with depth, particularly at higher frequencies (greater than 500 Hz). Conventional eddy currents typically do not respond to laminar discontinuities lying parallel to the surface [24]. Conductivity measurements have been used to detect poor process control [8]. Eddy current testing could be used to detect voids, depending on orientation, and possibly root flaws, depending on how tight the flaw is, but only for those defects which are close to the inspection surface.

Stepinski [16] reports that the use of ET for detection of LOP flaws within AA 2195 was successful for Marshall Space Flight Center (MSFC) and Lockheed Martin, specifically for detecting defects of at least 0.065 in in depth, using a 1 MHz pencil probe and a 300 kHz differential rotating probe. Depending upon plate thickness, the root-side of the plate may need to be accessible for in-service inspections.

3.1.1.4 Radiographic Testing

Radiography is readily capable of detecting volumetric defects in FS welds. Moles indicated that RT is difficult to use due to the large variety of defect orientations present in FS welds [8]; however, with a large defect size, RT can be very reliable. Detection of volumetric defects such as porosity, wormholes, and broken pin tool pieces would be its primary purpose.

It should be noted that Stepinski [16] reported film and digital radiographic inspection methods were successful on aluminum FS welds with a 90% probability and 95% confidence for detection of LOP flaws at Lockheed Martin [16]. The LOP flaws detected by radiographic inspection were approximately 30% of the material thickness or greater.

3.1.1.5 Ultrasonic Testing

Conventional UT is limited in its ability to detect defects with unusual orientations and skew [8], but in a detectable orientation, the U.S. Air Force has been able to find root flaw defects of about 0.050 in with UT [25]. Conventional UT could assist in the detection of defects such as porosity, wormholes, root flaws, and broken pin tool pieces.

Staniek et al. [26] used immersion ultrasonics to explore the adequacy of ultrasonics for detection of flaws in 4 and 6 mm thick FS welded aluminum alloy sheets. The authors used a high-frequency system to record A-, B-, C-, and D-scans at high resolution. Ultrasonic pulse-echo techniques (using a single transducer) and through-transmission techniques (using two transducers functioning as transmitters and receivers) were used at an incidence angle of 0º and 20º, as shown in Figure 15 and Figure 16. Figure 15 illustrates a schematic of the expected angle of incidence and reflection for volumetric and linear defect types with UT results from inspection of boreholes in fabricated test specimens. Figure 16 shows UT inspection results using 25 MHz transducer at 0º incidence for volumetric defects in 4 mm thick FS welded aluminum alloy. According to the authors, the best results were achieved using a 25 MHz broadband transducer. The results indicate that holes, pores and voids always offered a reflecting surface regardless of angle of incidence and that defects with planes along the welding direction and perpendicular to the surface, such as LOP, are detectable with a diagonal angle of incidence as illustrated in Figure 17. Figure 17 provides side-by-side comparison of ultrasonic C-scan inspection results of elliptically machined root-side defects using unfocused 10 MHz and focused 25 MHz transducers. Staniek et al. [26] determined that a focused sound transducer with an angle of entry or 20º in water is sufficient for investigating root gaps. Figure 18 shows a D-scan showing a root

defect that was not detectable via visual inspection. The authors summize that UT is suitable for routine FSW inspections of aluminum alloys and add that even the smallest crack may be detectable by conventional UT because of the high signal amplitudes reflected during their inspections.

3.1.2 Advanced NDE Methods

Because conventional NDE techniques cannot detect some of the defect types and orientations encountered in FSW, many industries have been trying to refine some newer NDE methods. The aerospace industry, probably having some of the smallest critical flaw sizes, has differing opinions on the current capabilities of these newer methods. The U.S. Air Force desires 90 to 95% probability of detection (POD) for flaws of 0.001 in or less [20]. The U.S. Air Force has focused on phased-array UT and Meandering Wandering Magnetometer (MWM)® ET but has been unsuccessful in achieving this POD goal to date. NASA has found phased-array UT to be excellent at detecting FSW defects and has implemented phased-array UT in production. NASA has had some difficulty detecting lack of adequate forging and kissing bond defects created with self-reacting pin tools, but have been completely successful at detecting defects created with fixed pin tools, when compared with the results of destructive testing [12], [15].

3.1.2.1 Phased-Array Ultrasonic Testing

Direct UT by back reflection does not reliably detect kissing bonds [27]. Table 2 shows some of the results using RT and UT on a number of welds made with induced flaws. Phased-array UT has the ability to change inspection angles and to skew the beam in order to inspect a location within the weld for defects of many different orientations [8].

André Lamarre, Olivier Dupuis, and Michael Moles of R/D Tech found the optimal angles to be 35º for inspecting the crown of the weld and both 35º and 65º for analyzing the root of the weld in order to maximize the probability of detection for FSW defects [7]. Table 3 shows the results of the group's analysis of detectability for various angles.

Phased-array UT can detect all internal volumetric defects in FS welds. Also, ultrasonic attenuation measurements can be utilized to detect whether the grain size is refined properly from adequate mixing [7].

NASA and Lockheed Martin have been able to evaluate and utilize phased-array UT in actual practice. Phased-array UT can be employed in sectorial scan mode, where a wide range of angles are inspected at the expense of inspection coverage area, or in linear scan mode, where a large coverage area is inspected at one particular angle. Studies have found a couple ideal angles for detecting FSW defects (see Table 3). NASA and Lockheed Martin have utilized a 45° angle in linear-scan mode to increase inspection speed, due to the ability to scan a wide swath of area on a single pass. Searching for flaws of 0.020 – 0.025 in or greater, the two organizations have met with complete success when confirmed with

destructive analysis. With the aid of phased-array UT, both Lockheed Martin and NASA have found tears, voids, LOP defects, and surface defects of 0.008 – 0.010 in or greater [12].

R/D Tech's phased-array UT technique is able to detect LOP defects equal to or greater than 25% – 30% percent of the materials thickness [16]. Kleiner and Bird [27] have optimized phased-array ultrasonic techniques for enhanced detectability and as a measure for process and quality control. The authors demonstrated that high frequency (20 MHz) focused probes are able to detect very small (less than 0.5 mm) LOP and kissing bonds in weld roots.

Although the work is in early development, Bird et al. [28] have developed a novel method for the detection of kissing bonds in butt welds based on backscattered noise analysis. Ultrasonic frequency measurements (for both butt and lap welds) have also been performed as a quality control technique. The basis for ultrasonic noise distribution measurements is to access the quality of the weld root by comparing the noise level at the weld root to that of the parent metal. Experimental trials on 6-mm thick 7xxx aluminum alloys were successfully demonstrated. Similarly, ultrasonic frequency measurements can measure frequencies of the weld nugget and the parent material and ultimately provide a weld quality indicator based on the normalized ratio. Experimental trials have shown that the weld metal and the base metal (or unstirred/undeformed metal under the nugget) exhibit drastic differences in frequencies (20 MHz vs. 8 MHz) such that root flaws become relatively and consistently distinguishable. The authors noted that little frequency contrast was found for AA 5083 lap welds.

3.1.2.2 Acoustic Emission

Chen's group explored the use of acoustic emission (AE) for monitoring the FSW process of Al 6061 to detect defects during manufacturing [21] and successfully used AE to locate intermetallic phases ($Al_{13}Fe_4$ and Al_5Fe_2) within the weld zone of FS welded AA 6061 and AISI 1018 steel [13]. Acoustic emission has already been proven for the monitoring of fusion or resistance weldments during welding and during the cooling period [24].

3.1.2.3 Multi-Element Eddy-Current

Lockheed Martin and NASA have worked with JENTEK Sensors Inc. to develop eddy-current methods for inspection of FS welds since 1998. JENTEK Sensors has demonstrated the feasibility of multi-element eddy-current sensors known as Meandering Wandering Magnetometer (MWM)® and MWM® arrays to aid in the detection of LOP defects [29]. Meandering Wandering Magnetometer® sensors are designed to measure the absolute electrical conductivity on the root side of the welded panel. Since microstructural changes occur within the weld nugget during FSW, its electrical conductivity also changes and is distinguishable from the unwelded (i.e., base metal and material not plasticized under the weld nugget creating an LOP condition). Work performed at NASA has demonstrated that a 1.14 mm LOP indication was identified by MWM®. Note that MWM® eddy current array probes have limited penetration, as with conventional eddy current

techniques, access to the root-side of the plate is required for inspection of the root. Meandering Wandering Magnetometer® exhibits good surface and near-surface detection, defect-sizing and characterization capability, with axial and circumferential discrimination [7].

3.1.2.4 Transient Eddy Current Inspection

Smith [30] discusses in his paper that unlike conventional eddy current inspection techniques that rely on continuous-wave high-frequency or low-frequency (down to approximately 500 Hz) eddy currents to measure near-surface electrical conductivity, transient (pulsed) eddy current inspection relies on time-dependence of the response to changes in conductivity (or integrated conductivity response) around the eddy currents. These changes in conductivity can be measured from defects such as voids and from smaller variations due to microstructural changes. In this paper, the author provides a general specification and requirements for in-situ transient eddy current inspection for FSW in-process monitoring. These specifications include scanning, temperature tolerance, data acquisition, probe design, thermal barrier design for probes, and system design. The advantages of transient eddy current as described by the author are the following:

- Improved depth of penetration (up to 12.5 mm depth) through the use of specially designed Hall sensors (versus coils used in conventional eddy current sensors)
- Improved spatial resolution through the use of Hall sensors
- Ability to map localized electrical conductivities in 3-D through the weld to detect changes in the process conditions
- Improved defect detectability as a function of depth
- Ability to correct for lift-off effects using a post-processing algorithm.

The author concludes from experimentation on plates with machined and actual defects on FS welded aluminum alloys (6.1- and 12.5-mm thick AA 2024, 12.5-mm thick AA 7449, and 12.5-mm thick AA 7010) eddy current transient inspection can successfully penetrate deep depths into the weld and provide 3-D maps of locations with changes in conductivity and can also provide a cross-sectional profile of a parameter (such as hardness) related to the electrical conductivity.

3.1.2.5 Holography & Shearography

Lobanov's group describes the potential of holography for FS welded aluminum, as well as electron speckle-interferometry and electron shearography, in determining residual stresses within components [31]. Of the methods, shearography is the most tolerant of vibration during the analysis [24].

3.1.3 Calibration Standards

In general, the industrial approach for fabricating calibration standards seems to include fabrication of FS welds of the same alloy and heat treatment to be manufactured and introducing machined defects such as EDM notches and side-drilled holes [12]. Some experimenters have successfully replicated defects that are not easily machined (such as kissing bonds) by producing sufficient oxides on the mating surfaces through heat treatment prior to FSW [32] which could then be used in a calibration standard.

3.2 Destructive Testing

Leonard stated that the only definitive method for confirming the presence of root flaws is by a destructive bend test with the root in tension [10]. While NASA has found success with phased-array UT for detecting root flaws, every industry surveyed employs extensive destructive testing on both test specimens created prior to welding of the final product and run-on/run-off tabs, cut from the production welds. The data gained on weld quality is an essential risk management method used on FS welds, due to the limited production experience and the developing understanding of the FSW process.

3.3 In-Process Monitoring

Once the shoulder plunge depth, tool rotation speed, and welding travel speed have been optimized for a particular FSW process, the resultant weld properties are highly repeatable due to the removal of the human element (the welder) from the process [3]. This is because the process is automated. For fixed pin tool 2xxx series aluminum welds, NASA and Lockheed Martin have not found any defects, outside their acceptance/rejection criteria, when welding within an optimized parameter envelope [12]. Making sure parameters stay within a pre-defined welding procedure process window helps to ensure quality welds are being produced for instances where destructive testing cannot be performed. Also, some advanced NDE methods can be utilized for in-process monitoring, such as AE (see section 5.1.2.3) and transient eddy current inspection (see section 5.1.2.5).

4 Industry Documents

4.1 Lloyd's Register of Shipping

Lloyd's Register of Shipping (LR) has constructed guidelines for the approval of FSW [11]. The guidelines apply only to aluminum butt welds from sheet, plate, and extrusion products. Also, the LR document instructs the reader to follow fusion welding guidelines, unless otherwise stated.

The LR guidelines state that the welding personnel are to be trained on FSW systems. Operators should be capable of adjusting the system, and should be able to identify failures in either the system or the welding process and take remedial action. Friction stir welding procedures are to specify:

- Alloy
- Temper
- Thickness
- Edge preparation
- Gap between plates
- Joint type
- Tool type
- Shoulder diameter & design
- Probe length, diameter, & design
- Operating angle
- Number of passes
- Rotation speed
- Down force & welding speed
- Post-weld dressing

The welding procedure requires qualification through fabrication of test coupons as seen in Figure 19. These test coupons undergo 100% examination.

Nondestructive examination includes visual examination (for cracks, porosity, LOP, excess flash, an acceptable-looking tool exit hole, an as-machined joint surface, and a clean joint root), dye penetrant examination on both the face and root of the weld, and radiography.

Destructive examination includes tensile tests, transverse face and bend tests (if a herring bone structure is present along the root, it may be machined prior to bending), and metallographic investigation of the weld structure with no evidence of porosity, lack of fusion, or inadequate penetration and exhibiting one central nugget. The document permits an oxide at the root of the weld, even if the oxide is cracked, as long as the root is unaffected.

Production may only start after the process is qualified. As far as weld preparation, the document only states to perform edge preparation similar to fusion welds. Production quality is controlled through first production welds (subject to visual and bend tests), and test coupons produced during fabrication (subject to full length NDE, transverse bend tests, transverse tensile tests, and macro sections) – all preferably taken from the production material run-on/run-off tabs. The document suggests that production test coupons should be generated every 100 m of weld length. The LR document allows the

use of VT, PT, and RT to be employed on production welds and there is an option for the use of UT. Also, in-process monitoring is considered essential for monitoring and adjusting the process parameters during welding to ensure that the weld is being made within the tolerance limits established within the welding process specification along its entire length. Any welds containing unacceptable porosity, cracking, or lack of fusion are allowed to be repaired by an FSW pass, if the repair process has been qualified.

4.2 NASA Process Specification for Friction Stir Welding

NASA's manned space program requires manufacturing processes to be performed with a high degree of reliability and repeatability. After a welding procedure is optimized, a large number of weld test samples are generated for mechanical testing. NASA uses the data to evaluate weld strength, quality, critical flaw size, and factors of safety. Due to the strict safety requirements, the mechanical data values have to have a 99% confidence level that 90% of the weld strength values fall within design criteria [3]. NASA utilizes a practice of recording the critical processing parameters, destructively testing the run-on/run-off tabs, and inspecting 100% of the weld in order to meet these requirements [15]. For NASA's external fuel tanks, which are FS welded, inspection is performed by conventional methods – visual, dye penetrant, film radiography, and ultrasonic – to the same requirements as fusion welds [3]; however, it cannot be understated that the tanks are only used for a single launch. Also, linear flaws of up to 0.75 inch are considered acceptable for class B welds (classification listed below) on the external tank [12]. Although film radiography is used in the detection of wormholes and larger, through-thickness, lack of forging flaws, phased-array UT is being utilized by NASA to detect these flaws and many of those much harder to find with RT or conventional UT. Using R/D Tech's Tomoview with 128-element transducers on the Space Shuttle's external tank, NASA has been able to detect embedded and near-surface flaws such as lack of adequate forging (similar to incomplete fusion in conventional welds), LOP (even with the root in compression), wormholes, surface galling, tears, and residual stresses [3].

NASA Process Specification for Friction Stir Welding, PRC-0014, provides the minimum requirements for FSW with respect to flight and non-flight hardware. NASA classifies welds into four categories, A – D. Class A welds are any non fail-safe load bearing components, Class B welds are any fail-safe load bearing parts, Class C welds are any non-critical minor load bearing components, and Class D welds are non-flight, non-critical parts.

The document specifies extensive NDE for Class A welds, including VT, PT, either RT or UT, and any alternate methods deemed appropriate. The NDE inspection requirements decrease rapidly from there, with Class B requiring only VT and PT, Class C only VT, and Class D only "to verify the type, nominal size, length, location, and that the welds were left in a condition exhibiting good workmanship practices" [33].

Another interesting weld classification instruction is the requirement for two welds that intersect, overlap, or even come within a 0.5 in or less in proximity, the lower class weld shall be upgraded to the same grade as the higher class weld and subject to the higher class inspection requirements [33]. At the time of this report, NASA and

Lockheed Martin are starting to evaluate the intersection of fusion welds with FS welds, and the detectabilty of linear porosity under the cap of the fusion weld over an FSW [12].

4.3 Other Industry Guidelines

Many of the guidelines, specifications, or standards used by industry in FSW are kept as proprietary information. In general, industry has found conventional NDE techniques unable to reliably locate every type of FSW defect, so a combination of conventional NDE techniques, in-process monitoring, and destructive testing are employed to reduce the risk [12], [15], [20]. Phased-array UT, one of the advanced NDE methods, has been extensively tested in an industrial setting and has shown the capability to identify FSW defects not detectable by conventional NDE methods. However, phased-array UT has yet to become a general practice.

5 Summary

The U.S. Navy is evaluating friction stir welding (FSW) for joining 5xxx and 6xxx aluminum alloys as an alternative to conventional arc welding processes. Friction stir welding provides many advantages over conventional welding, but it also has the potential to create new defects that have never been encountered in naval structures. The purpose of this report is to provide a review of available information on FSW defects and the nondestructive examination (NDE) methods currently used to detect these defects.

Friction stir welding has many defects and characteristics common to conventional welding, such as dimensional variation, porosity, and root flaws. There are many nondestructive means capable of detecting such flaws within conventional welds. Traditional NDE techniques may have difficulty detecting some of these flaws in FS welds, depending on (1) flaw size and orientation and (2) the unique microstructural characteristics of the FS weld. With NDE technique modifications, such as etching before PT and VT, and using immersion UT techniques as opposed to contact UT techniques, this survey indicated that traditional NDE techniques are generally being implemented successfully in detecting these flaws in FS welds. However, industry also includes various combinations of in-process monitoring, destructive testing, and newer NDE techniques, such as phased-array UT, to mitigate the risk of missing defects in hard to detect orientations or defects which may be small and detrimental to the weld properties.

Other flaws and weld characteristics, such as excessive flash, pin tool loss, wormholes, and kissing bonds are not seen in conventional arc welds. This review confirmed that most of these flaws are readily detectable through traditional NDE techniques. Of the FSW-specific defects, only the kissing bond cannot be reliably detected using conventional NDE techniques. Industry has depended upon various combinations of quality control, in-process monitoring, destructive testing, and newer NDE techniques such as phased array UT, in detecting these defects.

Although the kissing bond is the only flaw that cannot be reliably detected using conventional NDE techniques, this does not mean it is of any greater concern than the other types of flaws. Root flaws and wormholes can be just as detrimental, or more detrimental, than a kissing bond. It is also important to note that, while conventional NDE techniques can be utilized in searching for all but one of the FSW flaws, industry has found phased-array UT to be both capable in finding the most flaws with one method and possibly having the greatest ability of all the methods for detecting these FSW flaws.

The information gleaned from this survey indicates that the quality assurance approach generally used in current industrial applications of FSW may include some combination of conventional nondestructive inspection, in-process monitoring, destructive testing, and alternative nondestructive inspection methods, such as phased array ultrasonics. As with inspection of conventional arc welds, the inspection methods used for friction stir welds should be dictated by the specific requirements, for instance, intended structural application, criticality of the application, anticipated flaw types and flaw sizes, and the consequence of leaving undetected flaws in the structure.

References

[1] Threadgill, P.L., M.E. Nunn, "A Review of Friction Stir Welding: Part 1, Process Review", The Welding Institute (February 2003)

[2] Mishra, R.S., Z.Y. Ma, "Friction Stir Welding and Processing", Materials Science and Engineering R 50 (2005) 1-78, copyright Elsevier

[3] Ding, J., et al., "Friction Stir Welding Flies High at NASA", AWS Welding Journal (March 2006), 54-59

[4] Arbegast, W.J., "Friction Stir Welding After a Decade of Development", AWS Welding Journal (March 2006) 28-35

[5] Khaled, T., *An Outsider Looks at Friction Stir Welding, Report #ANM-112N-05-06*, Federal Aviation Administration (July 2005)

[6] Colligan, K.J., T.P. Creeden, *CVN-21 Concepts Exploration Project: Development of Friction Stir Welding for 5456-H116 Aluminum*, National Center for Excellence in Metalworking Technology (2005 August 5)

[7] Lamarre, A., O. Dupuis, M. Moles, "Complete Inspection of Friction Stir Welds in Aluminum using Ultrasonic and Eddy Current Arrays", 16th World Conference on NDT, Montreal, Canada (2004 August 30 – September 3)

[8] Moles, M., A. Lamarre, "Phased Array Ultrasonic Inspection of Friction Stir Welds", 4th International Symposium on Friction Stir Welding, Park City, Utah, USA (2003 May 14-16)

[9] Dickerson, T.L., J. Przydatek, "The Significance of Root Flaws in Friction Stir Welds in Aluminium Alloys", The Welding Institute (September 2000)

[10] Leonard, A.J., "Flaws in Aluminium Alloy Friction Stir Welds", TWI Core Research Report 726/2001, The Welding Institute (April 2001)

[11] *Guidelines for Approval of Friction Stir Welding*, Lloyd's Register of Shipping (2004 March 2)

[12] Suits, M., D. Cox, J. Leak, NASA Marshall Space Flight Center and Lockheed Martin, teleconference conversation (2006 April 25)

[13] Chen, C.M., R. Kovacevic, "Joining of Al 6061 Alloy to AISI 1018 Steel by Combining Effects of Fusion and Solid State Welding", International Journal of Machine Tools & Manufacture 44 (2004) 1205-1214

[14] Cox, D., J. Leak, NASA Marshall Space Flight Center and Lockheed Martin, teleconference conversation (2006 July 13)

[15] Suits, M., NASA Marshall Space Flight Center, telephone conversation (2006 April 21)

[16] Stepinski, T., et al., "Inspection of Copper Canisters for Spent Nuclear Fuel by Means of Ultrasound – NDE of Friction Stir Welds, Nonlinear Acoustics, and Ultrasonic Imaging", Svensk Kärnbränslehantering AB Technical Report TR-04-03 (January 2004)

[17] Sato, Y.S., et al., "Characteristics of the Kissing-Bond in Friction Stir Welded Al Alloy 1050", Materials Science and Engineering A 405 (2005), 333-338, copyright Elsevier

[18] Zhou, C., X. Yang, G. Luan, "Effect of Oxide Array on the Fatigue Property of Friction Stir Welds", Scripta Materialia 54 (2006), 1515-1520, copyright Elsevier

[19] Threadgill, P.L., "A Review of Friction Stir Welding: Part 2, Selection of Tool Materials", The Welding Institute (February 2003)

[20] Perkins, Larry, Wright-Patterson Air Force Base, telephone conversation (2006 April 19)

[21] Chen, C.M., R. Kovacevic, D. Jandgric, "Wavelet Transform Analysis of Acoustic Emission in Monitoring Friction Stir Welding of 6061 Aluminum", International Journal of Machine Tools & Manufacture 43 (2003) 1383-1390

[22] Fratini, L., B. Zuccarello, "An Analysis of Through-Thickness Residual Stresses in Aluminium FSW Butt Joints", International Journal of Machine Tools & Manufacture 46 (2006), 611-619

[23] Staron, P., et al., "Residual Stress in Friction Stir-Welded Al Sheets", Physica B 350 (2004) e491-e493

[24] *Nondestructive Testing Handbook, 2nd ed., Vol. 10 – Nondestructive Testing Overview*, American Society for Nondestructive Testing (1996)

[25] Tracy, N., Wright-Patterson Air Force Base, telephone conversation (2006 April 22)

[26] Staniek, G., W. Hillger, and C. Dalle Donne, "Ultrasonic Testing on Friction-Stir-Welded Aluminium Alloys", Welding and Cutting 6 (June 2002) 313-318

[27] Kleiner, D., C. Bird, "NDT Quality – Signal Processing for Stir Welding: The Dual Disciplines of Friction Stir Welding and Phased Array Ultrasonic Inspection are Combined in a Truly International Quality Assurance Project", Qualistir Consortium Bulletin

[28] Bird, C., "The Inspection of Friction Stir Welded Aluminium Plant", 5th International Friction Stir Welding Symposium, Metz, France (2004 September 14-16)

[29] Goldfine, N., et al., "Friction Stir Weld Inspection Through Conductivity Imaging Using Shaped Field MWM®-Arrays", Proceedings of the 6th International ASM Trends in Welding Conference (2003)

[30] Smith, R.A., "The Potential for Friction Stir Weld Inspection Using Transient Eddy Currents", Insight 47:3 (2005), 133-143

[31] Lobanov, L.M., et al., "Non-Destructive Quality Control and Determination of Residual Stresses in Elements and Members of Machine – Building Structures Using the Methods of Holography, Electron-Speckle-Interferometry and Shearography", AllPnD by NDT.net

[32] Vugrin, T., et al., "Root Flaws of Friction Stir Welds – An Electron Microscopy Study", Friction Stir Welding and Processing III, TMS (The Minerals, Metals & Materials Society) (2005)

[33] *Process Specification for Friction Stir Welding, PRC-0014, Rev B*, National Aeronautics and Space Administration (January 2005)

[34] Zhou, C., X. Yang, G. Luan, “Effect of Root Flaws on the Fatigue Property of Friction Stir Welds in 2024-T3 Aluminum Alloys”, Materials Science & Engineering A 418 (2006), 155-160, copyright Elsevier

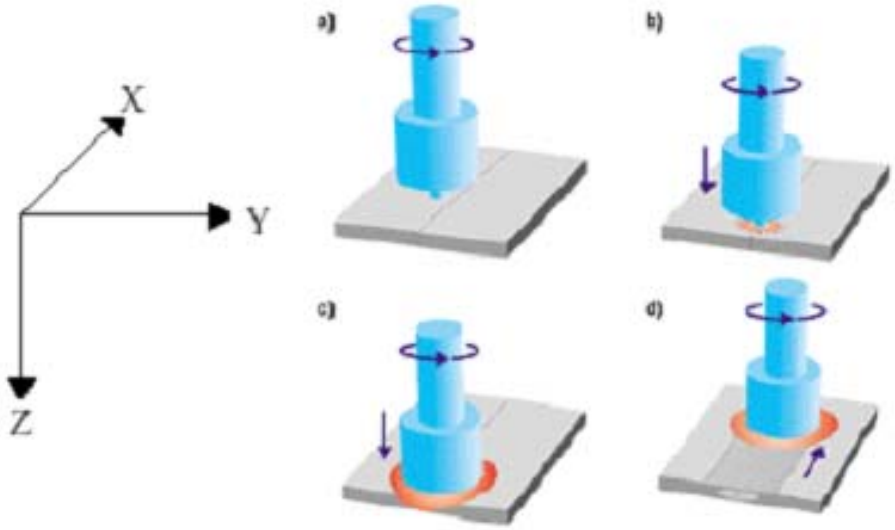

Figure 1. Schematic of FSW process sequence. (a) Rotating tool above joint; (b) Rotating tool lowered onto joint line; (c) Z-axis load drives rotating pin into the joint creating frictional heat; (d) X-axis load is applied causing the rotating tool to traverse along the joint line.

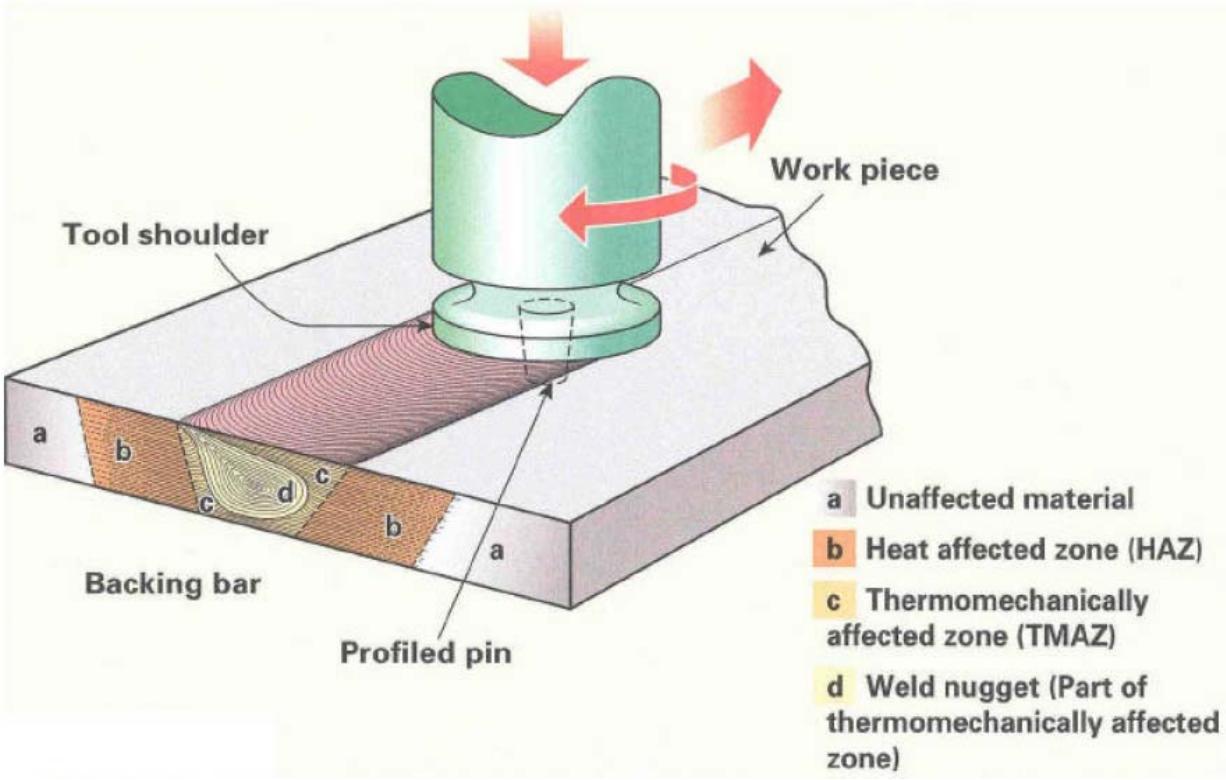

Figure 2. Some FSW terminology. Reproduced by permission TWI Ltd [10].

Figure 3. A 6mm thick AA 2014A FS weld cross-section. The increments at the bottom of the image are each 1mm. Reproduced by permission TWI Ltd [10].

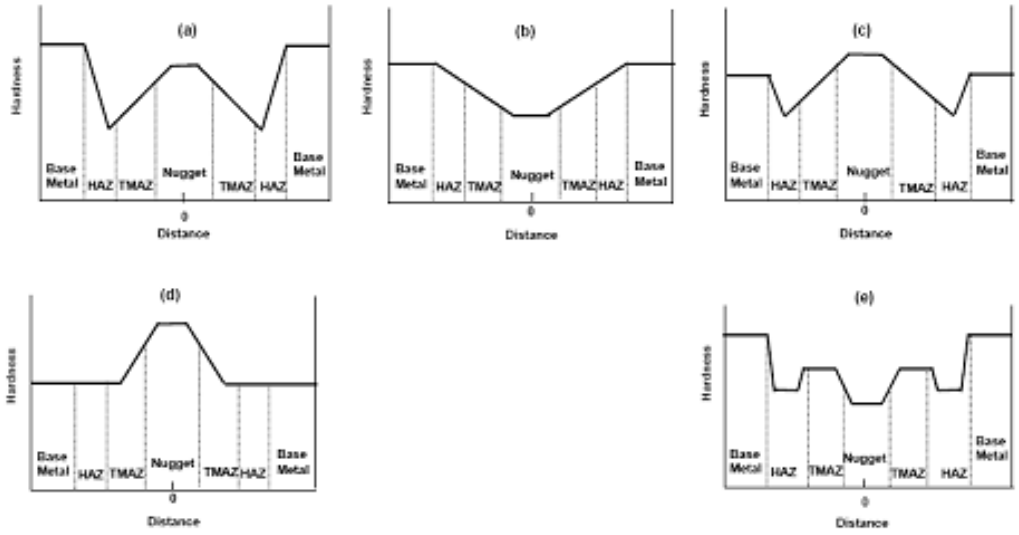

Figure 4. Some possible FSW hardness profiles along a given plane lying parallel to the crown and root of the weld. (b) schematically represents an FS welded AA 5083-H131 hardness profile and (d) schematically represents an FS welded AA 5083-O hardness profile [5].

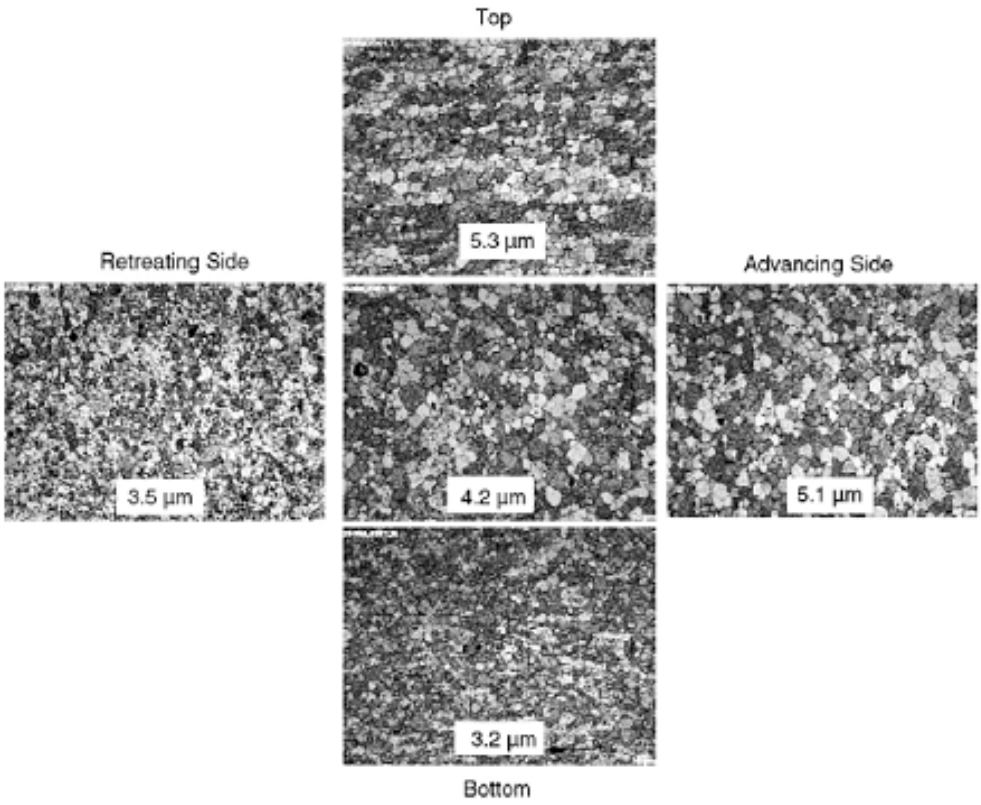

Figure 5. Grain size distribution at various locations within an AA 7050 weld nugget [2].

Figure 6. An FS welded aluminum alloy with excessive flash.

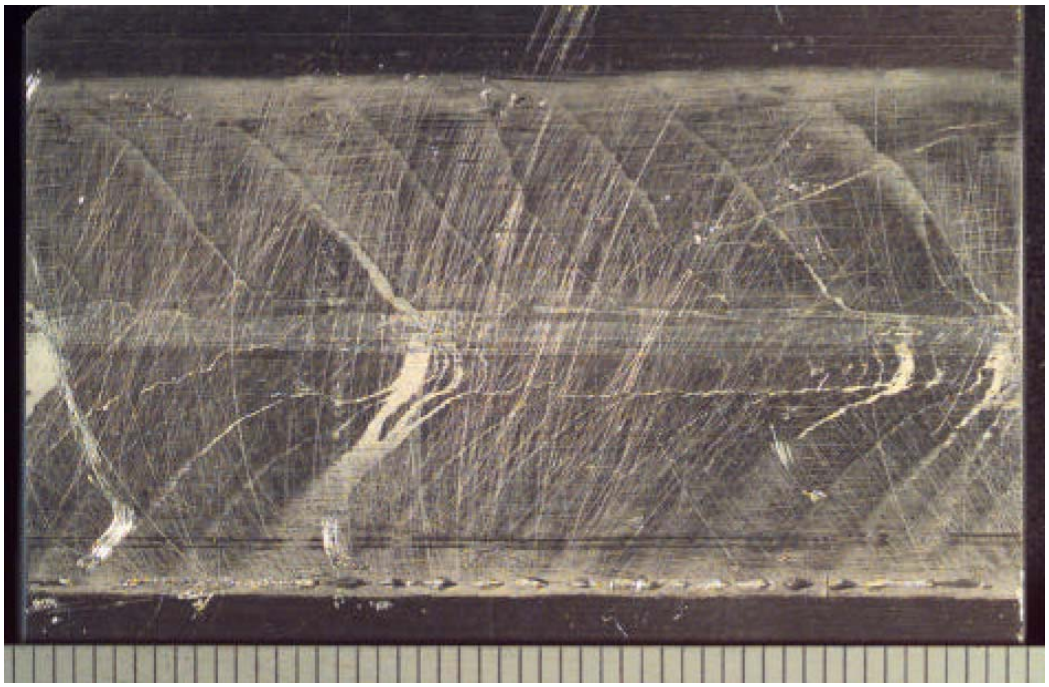

D617

Figure 7. Chevron markings found on the root side of an AA 5083 FS weld. 1mm increments run along the bottom of the image. Reproduced by permission TWI Ltd [10].

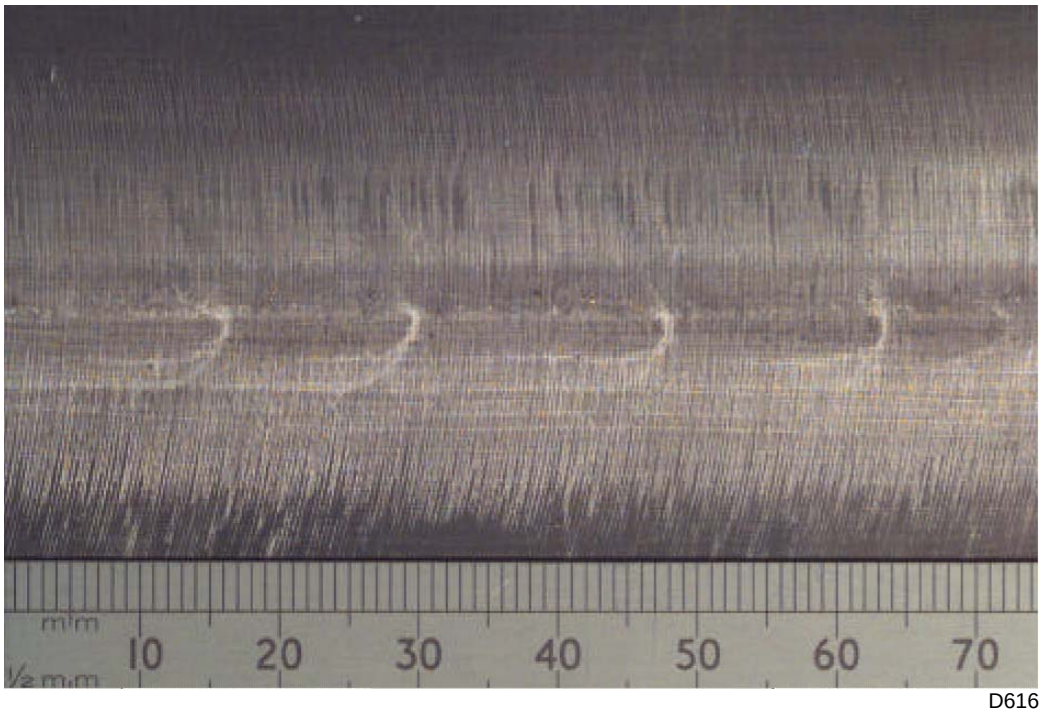

D616

Figure 8. Chevron markings found on the root side of an AA 5251 FS weld. 1mm increments run along the bottom of the image. Reproduced by permission TWI Ltd [10].

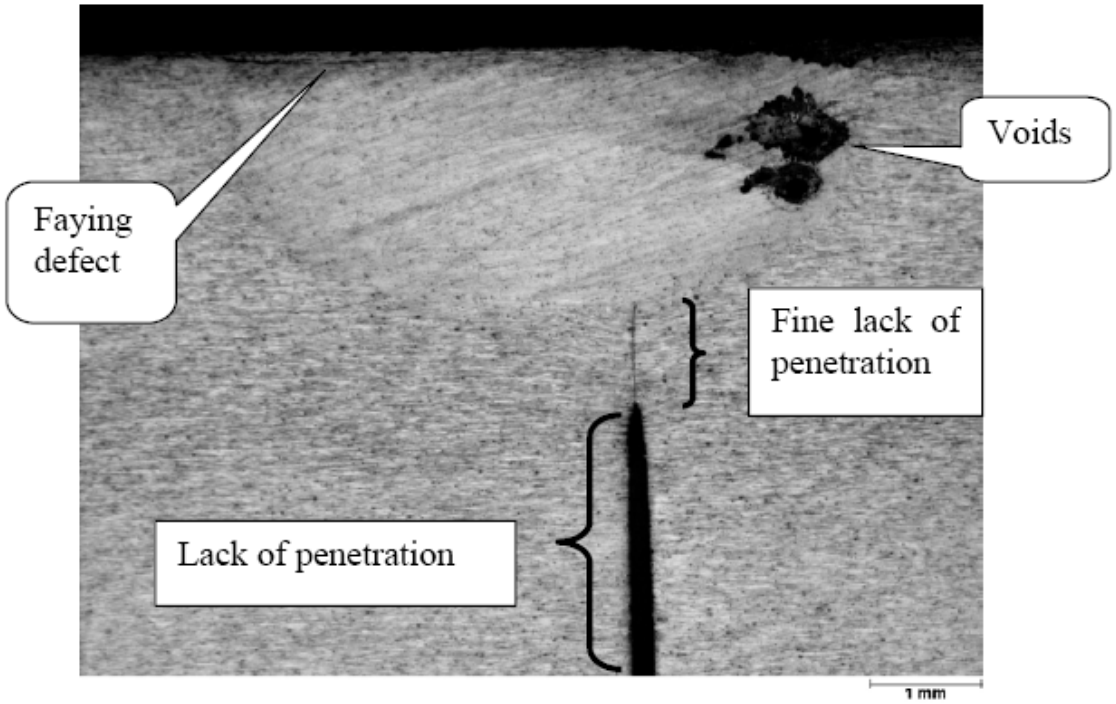

Figure 9. Macroscopic etch showing a faying surface defect, void, and LOP defect. Reproduced by permission TWI Ltd [28].

Figure 10. An FS welded aluminum alloy containing a surface-breaking wormhole defect.

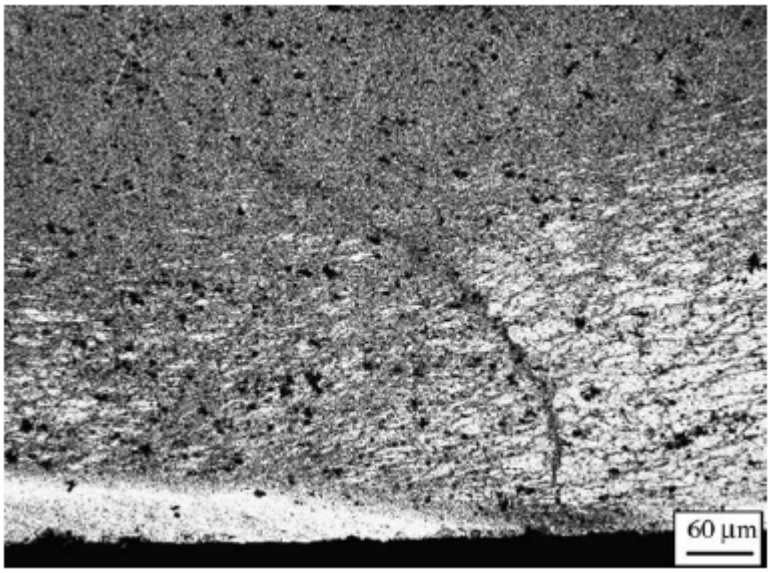

Figure 11. Optical micrograph of a root flaw in an AA 2024-T3 FS weld, after etching [34].

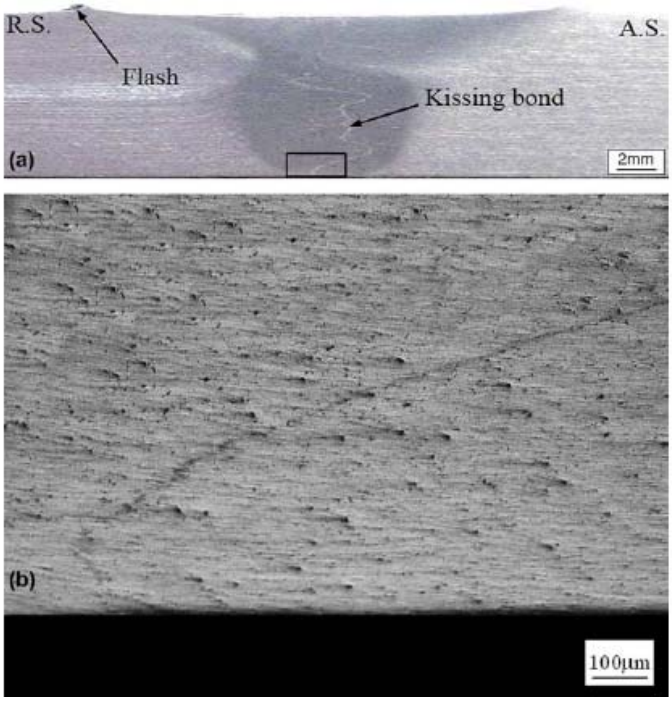

Figure 12. (a) Cross-section perpendicular to the welding direction of an etched AA 5083 FS weld and (b) an optical micrograph of the black-square region in (a). Notations "R.S." and "A.S." in (a) stand for "retreating side" and "advancing side" of the welding tool, respectively [18].

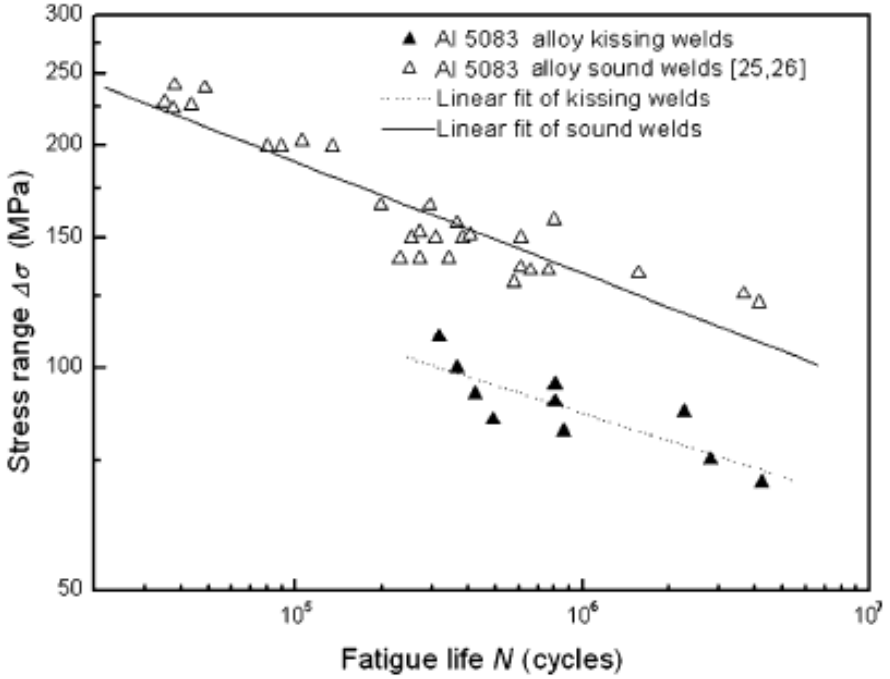

Figure 13. Fatigue data and corresponding S–N curves of AA 5083 kissing bonded and sound welds [18].

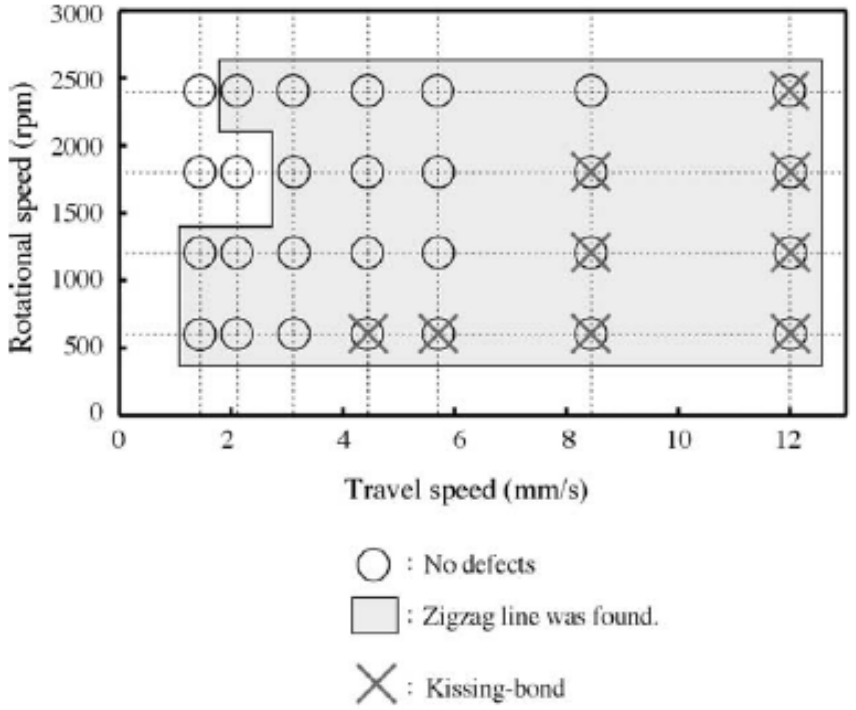

Figure 14. Effect of welding parameters on the formation of a visible zigzag line (upon etching) and kissing bond in an FSW AA 1050 weld [17].

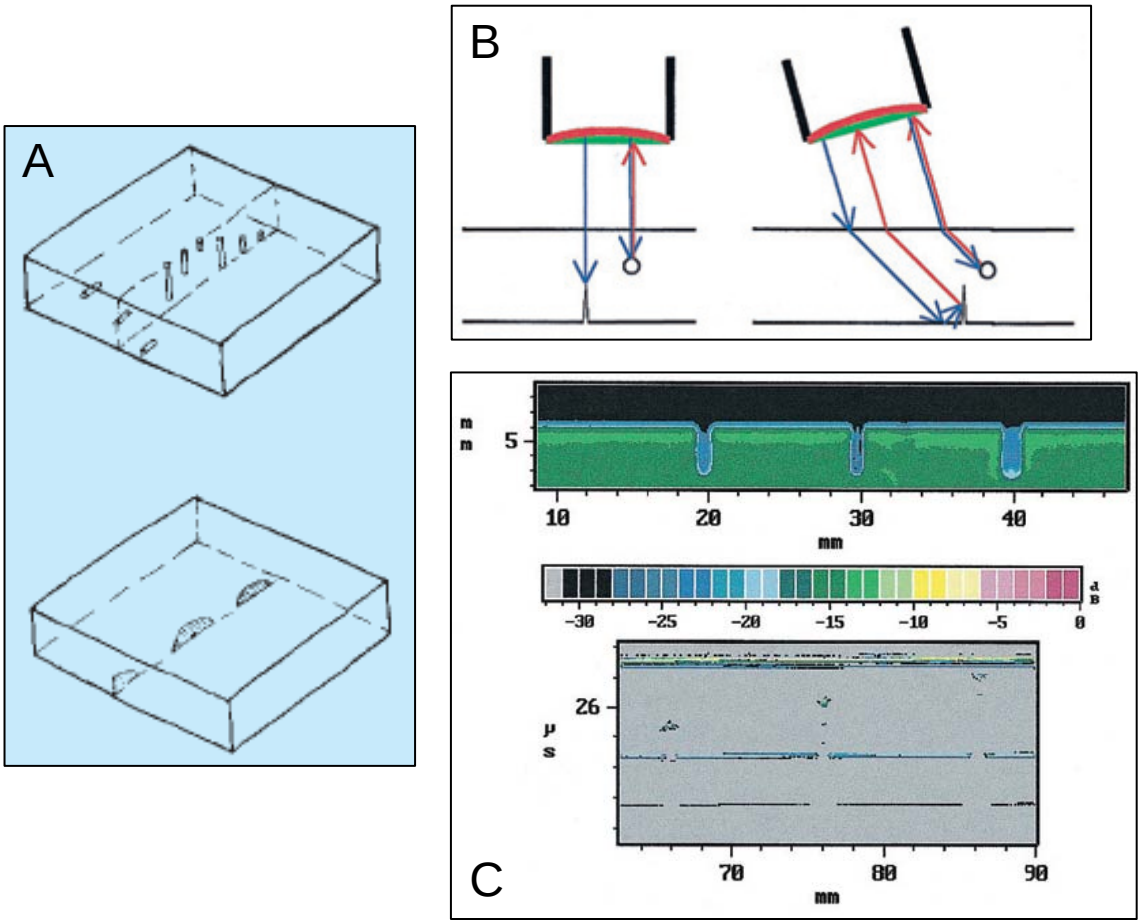

Figure 15. (A) Schematic showing test specimens created with known size and location for boreholes (top) and EDM notches representing elliptical cracks (bottom) within an aluminum alloy, (B) schematic showing 0º and 20º inspection angles (in water) evaluated for inspection of lack of penetration and volumetric defects, such as voids, and (C) showing (top scan) ultrasonic C-scan results for borehole echoes and (bottom scan) showing a B-scan (side view of the boreholes) [26].

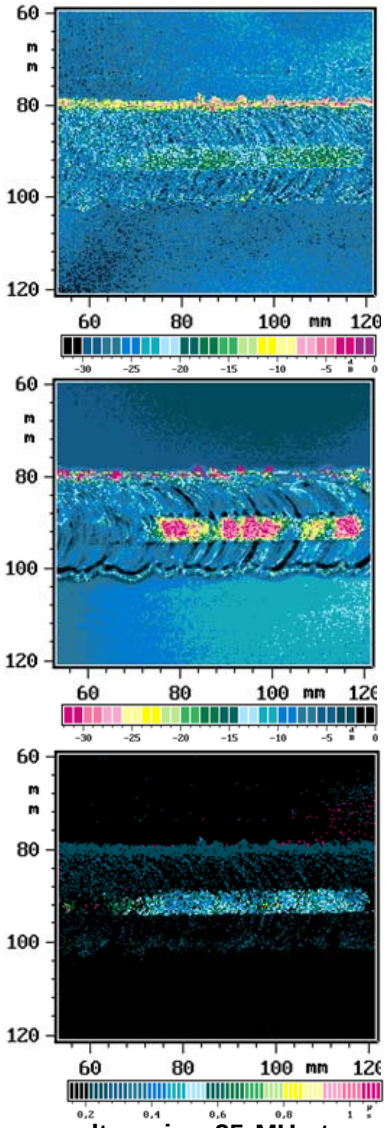

Figure 16. UT inspection results using 25 MHz transducer at 0º incidence of defects in 4-mm thick FS welded aluminum alloy - top: shows a C-scan of the defect echo, center: shows a C-scan of the backwall echo, and the bottom: shows a D-scan (time of flight) echo. From the signal amplitude in the D-scan above and information regarding sound velocity of longitudinal waves in this aluminum alloy (6100 m/s), the author was able to roughly position the volumetric defect within the upper half of the 4-mm thick plate [26].

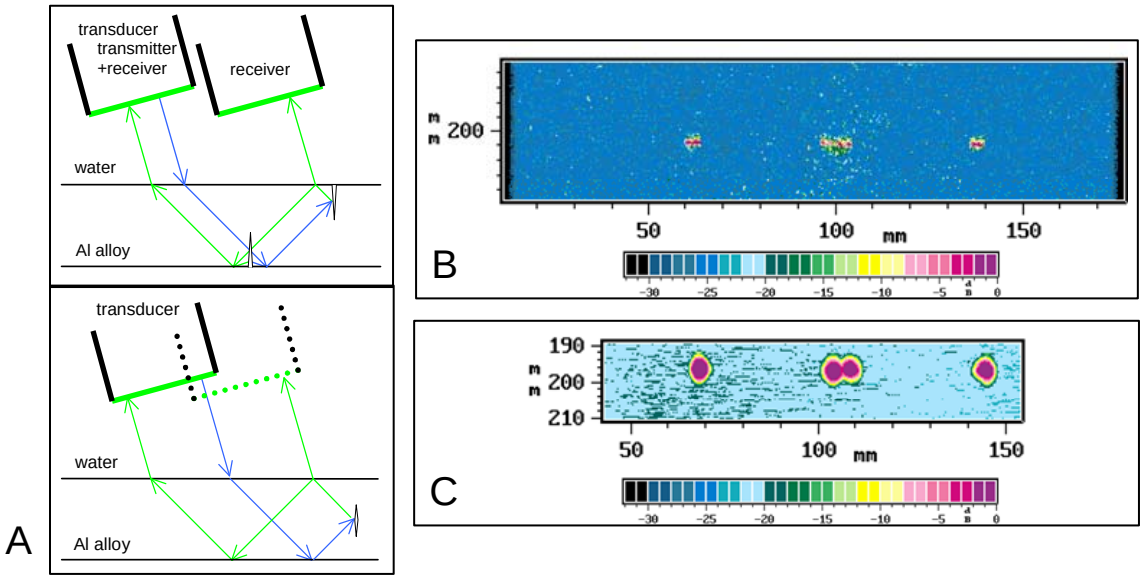

Figure 17. (A) Schematic showing two transducer configuration (transmitter/receiver and receiver) and a single transducer that transmits and receives; both using diagonal incidence (B) C-scan showing echo of elliptical crack in 6 mm thick aluminum plate using a *focused* 25 MHz transducer and a 20º angle of incidence in water (C) C-scan of same 6-mm thick aluminum plate but this time using an *unfocused* 10 MHz transducer at a 20º angle of incidence in water [26].

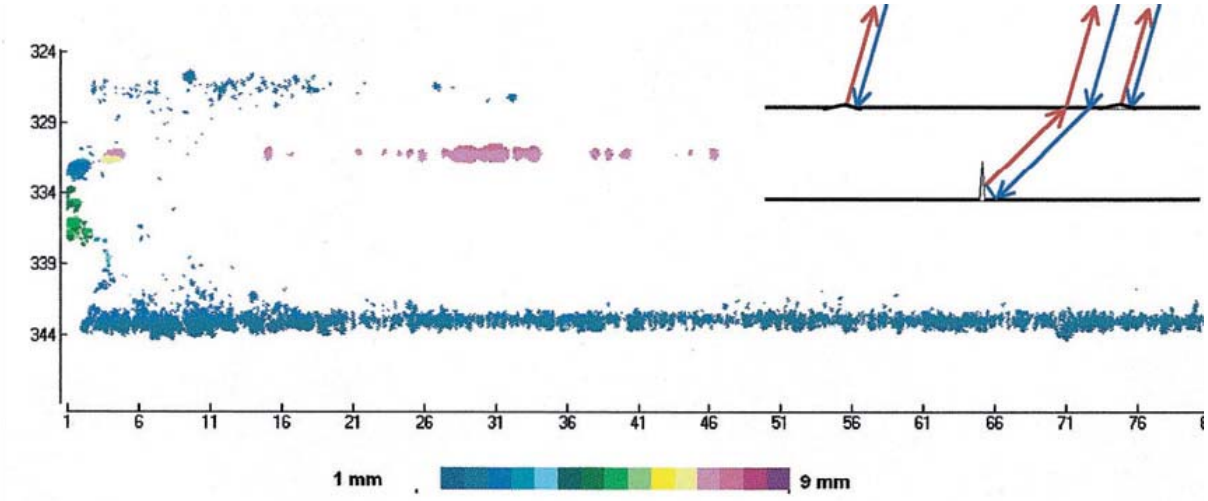

Figure 18. D-Scan (time-of-flight) showing a root gap detected by ultrasonic inspection in 6-mm thick aluminum alloy that was not detected by visual inspection. This scan was produced using a single focused 25 MHz transducer at an angle of 20º in water [26].

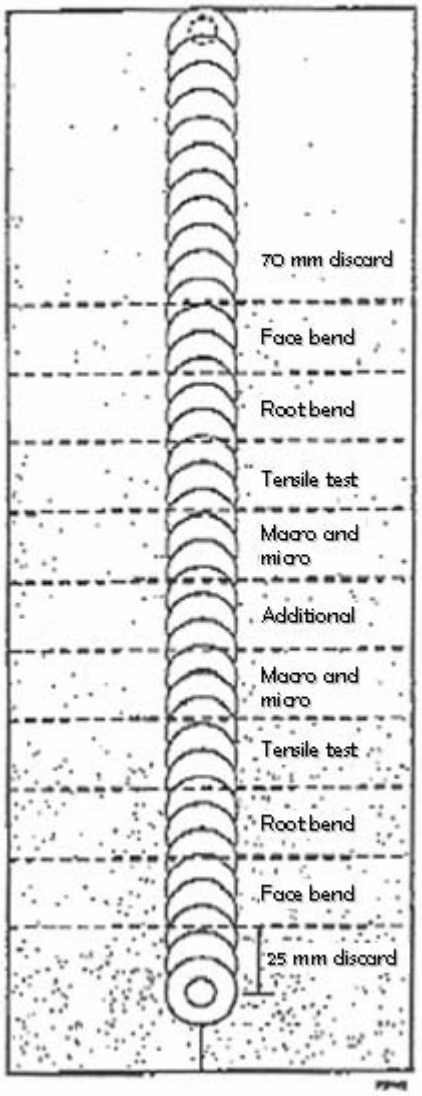

Figure 19. Locations of test coupons for qualification of welding procedures for LR's Guidelines for Approval of FS welds. Courtesy of Lloyd's Register [11].

Table 1. Key Benefits of FSW [2]

Metallurgical benefits	Environmental benefits	Energy benefits
Solid phase process Low distortion of workpiece Good dimensional stability and repeatability No loss of alloying elements Excellent metallurgical properties in the joint area Fine microstructure Absence of cracking Replace multiple parts joined by fasteners	No shielding gas required No surface cleaning required Eliminate grinding wastes Eliminate solvents required for degreasing Consumable materials saving, such as rugs, wire or any other gases	Improved materials use (e.g., joining different thickness) allows reduction in weight Only 2.5% of the energy needed for a laser weld Decreased fuel consumption in light weight aircraft, automotive and ship applications

Table 2. A summary of A.J. Leonard's x-ray and ultrasonic inspection results for each of the alloy 2014A FS welds. As can be seen when analyzing the columns, for many of the weld samples, RT and UT were unable to detect defects found through destructive analysis. Reproduced by permission TWI Ltd [10].

Weld	Other details	X-ray result	Ultrasonic inspection result	Sectioning results
W9	Shortened pin used	No defects recorded	No defects recorded	Root flaw
W10	2mm shim inserted between plates	No defects recorded	No defects recorded	No flaws found
W11	Total pressure limited to 500psi	Two large voids, 65mm and 140mm long	Two voids: No 1, 5mm deep, 45mm in length No 2, 4.9 to 5.6mm deep 120mm in length	Large voids on advancing side of the weld
W12	-	No defects recorded	No defects recorded	Root flaw - void beneath surface of weld
W13	-	No defects recorded	No defects recorded	No flaws found
W14	-	No defects recorded	No defects recorded	Small voids beneath surface of weld
W15	-	Large void and associated small voids at stop end of weld: area affected 85mm	Void 4.0m deep 11mm in length	Large void on advancing side of weld
W17	20µm anodised surface on plates	Feint linear indications full weld length	Intermittent reflector full weld length, 4.5mm deep	Oxide inclusions (joint line remnant)

Table 3. A qualitative summary of detectability of various defects at various angles using phased-array UT. As can be seen in this matrix, a combination of the 35° and 65° refracted angles would have been able to detect all the defects [7].

Refracted angle	35	40	45	50	55	60	65	70
Defect A side 1	2	2	5	5	10	10	10	8
Defect A side 2	4	4	4	6	8	10	10	8
Defect B side 1	2	2	2	5	5	8	8	10
Defect B side 2	2	2	2	5	5	8	8	10
Defect C side with lip	10	10	2	2	0	0	0	0
Defect C side opposite to the lip	10	8	5	5	0	0	0	0
Defects D-H for root defects	10	10	10	8	8	8	8	7

Distribution

	Copies
OFFICE OF NAVAL RESEARCH ATTN: ONR 03T (J. Carney) ONE LIBERTY CENTER 875 NORTH RANDOLPH STREET SUITE 1425 ARLINGTON, VA 22203-1995	2
COMMANDER ATTN: SEA 05P24 (Green, Mitchell, Wong, Nappi) NAVAL SEA SYSTEMS COMMAND 1333 ISAAC HULL AVENUE S.E. WASHINGTON NAVY YARD WASHINGTON, DC 20376	4
COMMANDER ATTN: SEA 05P2 (Qualley) NAVAL SEA SYSTEMS COMMAND 1333 ISAAC HULL AVENUE S.E. WASHINGTON NAVY YARD WASHINGTON, DC 20376	1
COMMANDER ATTN: SEA 05D NAVAL SEA SYSTEMS COMMAND 1333 ISAAC HULL AVENUE S.E. WASHINGTON NAVY YARD WASHINGTON, DC 20376	2
DEFENSE TECHNICAL INFORMATION CENTER 727 JOHN J KINGMAN ROAD SUITE 0944 FORT BELVOIR, VA 22060-6218	2

NSWC, CARDEROCK DIVISION INTERNAL DISTRIBUTION

Code	*Name*	*Copies*
60		1
61		1
611	Davis	1
611	DeLoach	1
611	Forrest	1
611	Liu	1
611	Posada	1
611	Trepal	1
611	Warren	1
611	Wolk	1
612	(Report Documentation Page)	1
613	(Report Documentation Page)	1
614	(Report Documentation Page)	1
615	(Report Documentation Page)	1
616	(Report Documentation Page)	1
617	(Report Documentation Page)	1
63	(Report Documentation Page)	1
65	(Report Documentation Page)	1
66	(Report Documentation Page)	1
3442	(TIC)	1


UNITED STATES NAVY
SURFACE WARFARE CENTER